Semiclassical Simulations of Azomethane Photochemistry in the Gas Phase and in Solution

ARTICLE *in* JOURNAL OF THE AMERICAN CHEMICAL SOCIETY · SEPTEMBER 2001

Impact Factor: 12.11 · DOI: 10.1021/ja0102843 · Source: PubMed

2 AUTHORS, INCLUDING:

Maurizio Persico
Università di Pisa
153 PUBLICATIONS **6,248** CITATIONS

SEE PROFILE

Semiclassical Simulations of Azomethane Photochemistry in the Gas Phase and in Solution

Paola Cattaneo and Maurizio Persico*

Contribution from the Dipartimento di Chimica e Chimica Industriale, Università di Pisa, via Risorgimento 35, I-56126 Pisa, Italy

Received February 1, 2001. Revised Manuscript Received May 11, 2001

Abstract: We present semiclassical simulations of the dynamical events which follow the $n \rightarrow \pi^*$ excitation of an azomethane molecule: decay to the ground state, isomerization, and dissociation. Ab initio potential energy surfaces and couplings, slightly modified according to available experimental data, are employed in conjunction with a trajectory-surface-hopping method. For an isolated molecule, we show that dissociation takes place in the ground state, because the radiationless decay is very fast. The dissociation is mainly sequential: the methyldiazenyl radical first produced fragmentates very rapidly to $N_2 + CH_3^{\bullet}$. The results of previous experiments by Lee's and Zewail's groups, from which partially conflicting conclusions had been drawn, are reproduced and interpreted. Molecular dynamics, coupled to the surface-hopping algorithm, allows us to simulate the photochemistry in acqueous solution. Here the fragmentation is suppressed because of vibrational energy loss to the solvent: only the isomerization takes place.

1. Introduction

The photochemistry of azoalkanes[1] poses some interesting problems. Taking azomethane as the chief example, irradiation in the $n \rightarrow \pi^*$ band (300 to 380 nm) in the gas phase produces fragmentation to $N_2 + 2CH_3^{\bullet}$ (a suitable source of methyl radicals). In solution, with several different solvents, cis−trans isomerization is the only important photoreaction, the dissociation being almost completely suppressed. The electronic surfaces on which these reactions take place (S_1, T_2, T_1, or S_0) have been the subject of contrasting interpretations. The mechanism of dissociation may be stepwise (or sequential), with production of a labile methyldiazenyl radical:

$$CH_3NNCH_3 \xrightarrow{h\nu} CH_3NN^{\bullet} + CH_3^{\bullet} \quad (1)$$

$$CH_3NN^{\bullet} \rightarrow N_2 + CH_3^{\bullet} \quad (2)$$

or it may be concerted, with a symmetric elongation of both N−C bonds:

$$CH_3NNCH_3 \xrightarrow{h\nu} N_2 + 2CH_3^{\bullet} \quad (3)$$

A continuum of intermediate hypotheses can be envisaged: in the sequential mechanism, the lifetime of $CH_3NN^{\bullet}$ can be as short as a few vibrational periods, with complete fragmentation following very closely the breaking of the first N−C bond; on the other hand, the concerted mechanism may be asymmetric, with different elongations of the two N−C bonds.

CARS measurements with nanosecond resolution on rotationally thermalized photodissociation products revealed the presence of vibrationally hot $CH_3^{\bullet}$ radicals, followed by colder $CH_3^{\bullet}$ with a delay of about 5 ns; this was interpreted as an evidence of stepwise dissociation, although no $CH_3NN^{\bullet}$ was detected.[2,3] In later experiments by Lee's group,[4] the photolysis was done in collisionless conditions, with exciting wavelength $\lambda = 351$ nm; the observed vector correlation between the methyl velocities put an upper bound to the lifetime of $CH_3NN^{\bullet}$, which should be significantly shorter than its rotational period (about 1 ps). Because the methyl kinetic energy distribution was found bimodal, the symmetric concerted mechanism could be discarded. A substantial confirmation of these findings came from independent measurements of the methyl fragment velocities, obtained by photodissociation with $\lambda = 333$ nm, and interpreted on the basis of a barrier impulsive model.[5] Lee's group further refined their experiments[6] by measuring the methyl kinetic energies for specific vibrational modes, with exciting wavelengths of 355 and 330 nm. Using time-of-flight mass spectroscopy with femtosecond time resolution, Zewail's group was recently able to detect the $CH_3NN^{\bullet}$ intermediate;[7] using $\lambda =$ 310 nm, its rise time (equal to the decay time of excited azomethane) was found to be 70 ± 10 fs, and its decay time 100 ± 20 fs. This is partially at variance with Lee's group finding, that the overall velocity distribution of $CH_3^{\bullet}$ velocities is isotropic, a fact that was explained by the long lifetime of the parent azomethane molecule.[4]

Ab initio calculations by Morokuma's group[8] and by ours[9−11] show that a conical intersection between the S_0 and S_1 potential energy surfaces (PES) is energetically accessible after vertical excitation. The S_1 PES has a twisted minimum, and even if the crossing seam probably does not intersect the minimum energy path for cis−trans isomerization,[11] the energy of the underlying

(1) Engel, P. S. *Chem. Rev.* **1980**, *80*, 99.
(2) Burton, K. A.; Weisman, R. B. *J. Am. Chem. Soc.* **1990**, *112*, 1804.
(3) Andrews, B. K.; Burton, K. A.; Weisman, R. B. *J. Chem. Phys.* **1992**, *96*, 1111.
(4) North, S. W.; Longfellow, C. A.; Lee, Y. T. *J. Chem. Phys.* **1993**, *99*, 4423.
(5) Fairbrother, D. H.; Dickens, K. A.; Stair, P. C.; Weitz, E. *Chem. Phys. Lett.* **1995**, *246*, 513.
(6) Bracker, A. S.; North, S. W.; Suits, A. G.; Lee, Y. T. *J. Chem. Phys.* **1998**, *109*, 7238.
(7) Diau, E. W.-G.; Abou-Zied, O. K.; Scala, A. A.; Zewail, A. H. *J. Am. Chem. Soc.* **1998**, *120*, 3245.
(8) Liu, R.; Cui, Q.; Dunn, K. M.; Morokuma, K. *J. Chem. Phys.* **1996**, *105*, 2333.
(9) Cattaneo, P.; Persico, M. *Chem. Phys.* **1997**, *214*, 49.
(10) Cattaneo, P.; Persico, M. *Chem. Phys. Lett.* **1998**, *289*, 160.
(11) Cattaneo, P.; Persico, M. *Theor. Chem. Acc.* **2000**, *103*, 390.

10.1021/ja0102843 CCC: $20.00
Published on Web 07/13/2001

Chart 1

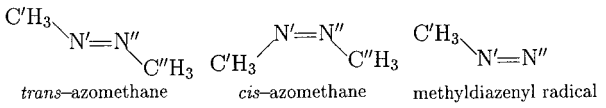

S_0 state is very close to that of S_1 in a wide region at CNNC torsion angles around 90°: as a result, fast radiationless transitions between the two states may take place at such geometries, as confirmed by preliminary calculations of the nonadiabatic dynamics.[10]

In this paper we present complete simulations of the photodissociation dynamics, performed within a semiclassical trajectory surface hopping (TSH) scheme. PES and couplings were computed by ab initio methods[9−11] and slightly modified for a better agreement with the available experimental data. The aim is to describe the mechanism in detail (electronic states involved in each step, concerted versus sequential bond breaking, dissociation versus isomerization). The surface hopping has been combined with a Molecular Dynamics model to run simulations of the azomethane photochemistry in aqueous solution. In this way we can compare in vacuo and condensed phase dynamics and analyze the caging mechanism. Details of the techniques have been given elsewhere;[12−14] here we shall concentrate on the description of the photoreaction dynamics, with a short account of the methods and of the potential energy surfaces.

2. Potential Energy Surfaces of Azomethane

Preliminary geometry optimizations for minima and transition states in S_0 and S_1 were performed at the CASSCF level with the 6-31G* basis set. With the help of these results, we selected about 260 geometries for single point calculations; five skeletal coordinates (R_1, R_2, ∠N″N′C′,∠N′N″C″, and ∠CNNC, see Chart 1) were varied independently; and the methyl internal coordinates were adjusted as functions of the other ones, on the basis of the CASSCF optimization results. A few more calculations yielded the necessary parameters for simple potential functions of the methyl coordinates (torsion, harmonic bends and stretches, umbrella motion).

The single point calculations were performed by the multireference perturbation CI technique CIPSI,[15−18] with selected zero-order determinantal subspaces, built over state-average CASSCF molecular orbitals. The electronic wave functions were transformed to a quasi-diabatic representation[19,20] by a technique based on maximum overlap with diabatic templates.[9,21,22] The eigenvalues of the electronic Hamiltonian **H** in the quasi-diabatic basis are the adiabatic PES, and the derivatives of its eigenvectors with respect to nuclear coordinates yield a convenient approximation for the nonadiabatic couplings which are needed to calculate radiationless transition probabilities. The H_{IJ} matrix elements have a much more regular behavior than the adiabatic potential energy functions and nonadiabatic couplings in the proximity of conical intersections; therefore, they could be fitted by analytic functions of the skeletal coordinates, taking into account the overall symmetry of the nonrigid molecule and of the two electronic states of interest. Finally, we applied corrections to the diagonal matrix elements, based on experimental data and on calculations of higher accuracy (6-311G** basis set, natural orbital CI with larger multireference spaces) performed at selected geometries; at this stage, the zero-point energy correction was also included in the PES, as our aim was to run semiclassical simulations where the ZPE would not be taken into account.

Potential energy maps and numerical data of the S_0 and S_1 surfaces, along with details of the computational procedure, were given in a previous paper.[11] Figure 1 summarizes our findings. The cis and trans isomers can be interconverted, preferably by inversion of one N atom in S_0 and by torsion of the N═N double bond in S_1. The minimum in the S_1 PES is located at a twisting angle ∠CNNC ≃ 130°. At ∠CNNC ≃ 90°, along the minimum energy path in S_1, the energy gap with respect to S_0 is less than 4 kcal/mol. From this geometry, to reach the lowest point on the crossing seam, one must slightly shorten the R_{NN} and R_{NC} distances, with a modest increase of the S_1 energy (about 2 kcal/mol).

The dissociation of one N−C bond, starting from the cis or trans isomer, goes practically without barriers, and requires 40.5 or 48.4 kcal/mol, respectively. The methyldiazenyl radical further dissociates with an activation energy of 11.1 kcal/mol. The symmetric (D_{2h}) simultaneous dissociation of both N−C bonds in *trans*-CH_3NNCH_3 goes through a barrier of 64.9 kcal/mol, although the complete fragmentation products are much lower in energy (31.6 kcal/mol with respect to *trans*-CH_3NNCH_3), and also more stable than $CH_3NN^{\bullet} + CH_3^{\bullet}$ (48.4 kcal/mol). Starting from *cis*-CH_3NNCH_3 the symmetric (C_{2v}) dissociation barrier is only slightly lower (60 kcal/mol). Our original ab initio results,[11] as well as those outlined above, which incorporate empirical corrections of a modest entity, are generally in good agreement with earlier computational findings.[7,8,23,24] The largest discrepancies arise about the symmetric dissociation barrier of *trans*-CH_3NNCH_3 and the activation energy of $CH_3NN^{\bullet}$, which are substantially lower according to Morokuma's[8] and Schaefer's[23] calculations; however, notice that their treatments underestimate also the complete fragmentation energy.

3. Semiclassical Method

We used two distinct but closely related methods, TSH (Trajectory + Surface Hopping) and MDSH (Molecular Dynamics + Surface Hopping), for the simulation of the azomethane photochemistry in vacuo and in solution, respectively. Both methods are semiclassical in that the nuclei follow classical trajectories on the adiabatic PES, but the electronic time-dependent Schrödinger equation (TDSE) is solved to calculate radiationless transition probabilities. At every time step along the trajectory, the electronic wave function is expanded in the set of the adiabatic wave functions ψ_K:

$$\Psi(t) = \sum_K A_K(t)\, \psi_K(\mathbf{Q}(t)) \qquad (4)$$

where $\mathbf{Q}$ is the collection of the nuclear coordinates. The $A_K(t)$ coefficients are obtained by solving the TDSE; to this aim, we switch

(12) Cattaneo, P.; Persico, M.; Tani, A. *Chem. Phys.* **1999**, *246*, 315.
(13) Ferretti, A.; Granucci, G.; Lami, A.; Persico, M.; Villani, G. *J. Chem. Phys.* **1996**, *104*, 5517.
(14) Cattaneo, P.; Persico, M. *J. Phys. Chem. A* **1997**, *101*, 3454.
(15) Huron, B.; Malrieu, J.-P.; Rancurel, P. *J. Chem. Phys.* **1973**, *58*, 5745.
(16) Cimiraglia, R. *Int. J. Quantum Chem.* **1996**, *60*, 167.
(17) Angeli, C.; Cimiraglia, R.; Persico, M.; Toniolo, A. *Theor. Chem. Acc.* **1997**, *98*, 57.
(18) Angeli, C.; Persico, M. *Theor. Chem. Acc.* **1997**, *98*, 117.
(19) Pacher, T.; Cederbaum, L. S.; Köppel, H. *Adv. Chem. Phys.* **1993**, *84*, 293.
(20) Persico, M. In *Encyclopedia of Computational Chemistry*; Schleyer, P. v. R., Allinger, N. L., Clark, T., Gasteiger, J., Kollman, P. A., Schaefer, H. F., III, Schreiner, P. R., Eds.; Wiley: Chichester, 1998.
(21) Persico, M. In *Spectral Line Shapes*; Rostas, F., Ed.; De Gruyter: Berlin, 1985; Vol. 3, p 587.
(22) Cimiraglia, R.; Malrieu, J.-P.; Persico, M.; Spiegelmann, F. *J. Phys. B* **1985**, *18*, 3073.
(23) Hu, C.-H.; Schaefer, H. F., III *J. Phys. Chem.* **1995**, *99*, 7507.
(24) Vrábel, I.; Biskupič, S.; Staško, A. *Theor. Chim. Acta* **1997**, *95*, 201.

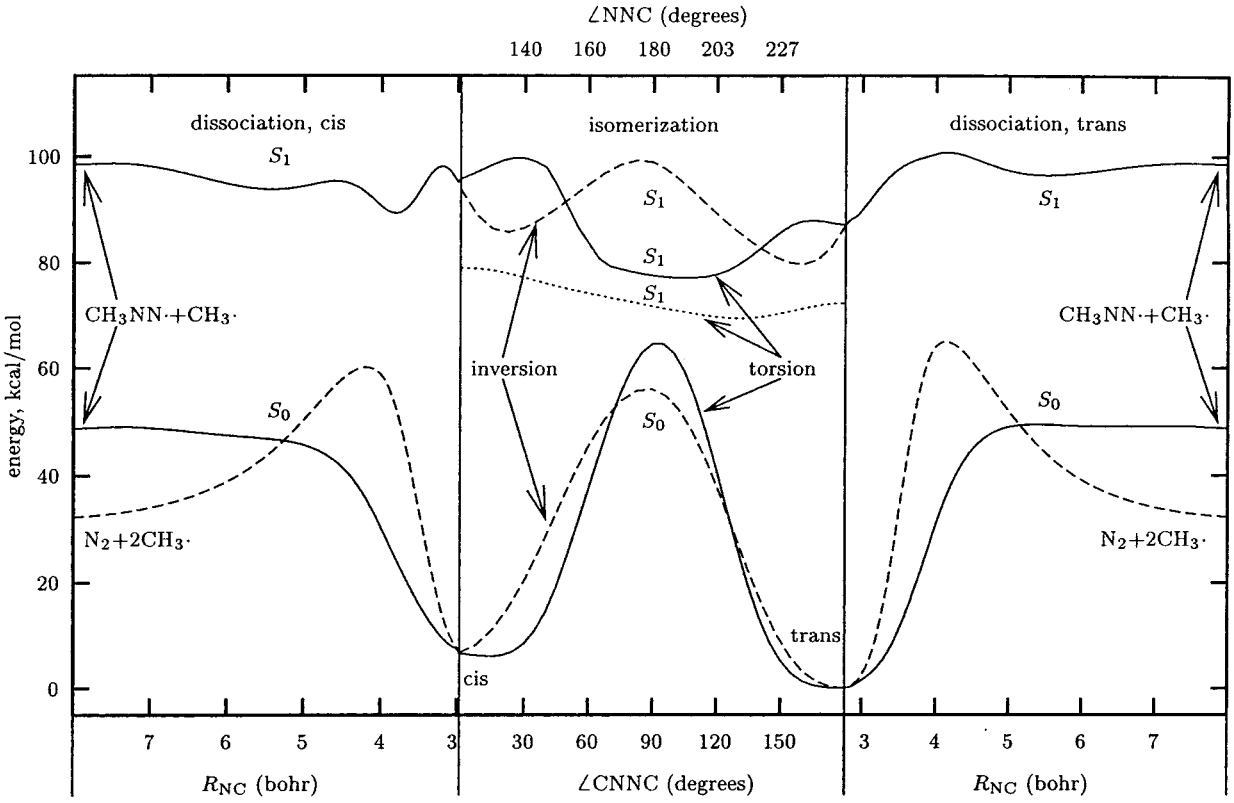

Figure 1. Potential energy curves of azomethane. Central panel: Isomerization by torsion of the N=N double bond (∠CNNC coordinate, bottom scale) or by planar inversion at one N atom (∠NNC coordinate, top scale); full lines, torsion, S_0 and S_1 energies with all internal coordinates except ∠CNNC optimized in the S_0 PES; dashed lines, inversion, all internal coordinates except ∠NNC optimized in S_0; dotted line, torsion, S_1 optimized energy. Left panel: Full lines, dissociation of one N−C bond for the cis isomer; dashed lines, symmetric dissociation of both N−C bonds. Right pane: Same for the trans isomer; all coordinates, except one (or both) R_{NC}, are optimized in the S_0 PES.

to the quasi-diabatic basis $\{\eta_I\}$, expanding $\Psi(t)$ as

$$\Psi(t) = \sum_I D_I(t)\, \eta_I(\mathbf{Q}(t)) \tag{5}$$

and we propagate in time the D_I coefficients; then, we obtain the $A_K(t)$ coefficients by the transformation $\mathbf{A} = \mathbf{U}^t\mathbf{D}$, where U is the matrix of the eigenvectors of the diabatic **H**. Only the matrix **H**(**Q**) is needed to solve the TDSE in this way, while the direct integration in the adiabatic basis[13,14] requires the dynamic couplings $\langle\psi_K|\partial/\partial Q_r|\psi_L\rangle$, in turn computed from **H** through the diabatic approximation.[9] Notice that the diabatic representation is introduced only to facilitate the fitting of PES and couplings and the integration of the TDSE in surface crossing situations, but the nuclear motion is determined by the adiabatic PES, and the electronic state probabilities are always expressed in the adiabatic representation. Along a single trajectory, the probability of the Kth state is $P_K(t) = |A_K(t)|^2$. Transitions from the current PES to another one are determined by changes in the P_K values, according to Tully's "fewest switches" surface hopping algorithm.[25,26]

For the isolated molecule simulations (TSH method), a swarm of 500 trajectories is run, with a Boltzmann distribution of initial conditions in the ground state; this is obtained by integrating Langevin's equation in the S_0 PES, and sampling nuclear coordinates **Q** and momenta **P** at regular intervals of time; for each set of initial conditions, a vertical transition is made (change of PES at fixed **Q** and **P**), the brownian interactions are switched off, and the regular TSH algorithm is started. Electronic state populations are obtained as fractions of the total number of trajectories which are on each PES at a given time; observables can be computed as averages over many trajectories.

In the MDSH method[11] for the simulation of nonadiabatic dynamics in the condensed phase, the purely classical part of the system, i.e., the solvent in the present case, is represented as in Molecular Dynamics, with standard intra- and intermolecular potentials. In this work, we adopted the flexible SPCE model for water.[27,28] We imposed periodic boundary conditions with Ewald's treatment of the Coulombic interactions. Each cell, of cubic shape with sides of 29.3 bohr, contained 120 molecules of water and one of azomethane. The semiclassical subsystem ("solute") interacts with the solvent through potential functions which are added to the diagonal matrix elements of the diabatic Hamiltonian **H**. In principle, the solute−solvent interaction potentials could be state specific (one for each diabatic state of the solute), so as to take into account solvent effects on the adiabatic wave functions and on the location of crossing seams, not only on the general shape of the PES. However, as in this work we are essentially interested in solute−solvent energy transfers, we adopt the same interaction potential for both states, using Jorgensen's BOSS parameters[29] for Lennard-Jones interatomic potentials (no Coulomb interactions between azomethane and water are included). The system is equilibrated in the ground-state PES for a sufficiently long time, then at regular time intervals a vertical excitation to S_1 gives origin to a trajectory: thus a swarm of 100 trajectories with stochastically chosen initial conditions is generated, in this case without resorting to brownian dynamics.

Tully's surface hopping algorithm,[25,26] which is incorporated in both the TSH and MDSH strategies, aims at distributing the classical trajectories over the electronic states according to the state probabilities P_K, which are derived from the TDSE. A disagreement between the fraction of trajectories in state K, N_K, and the average of P_K over all trajectories, $\langle P_K\rangle$, may arise, mainly because of classically forbidden surface hoppings. These are the nonadiabatic transitions which should occur according to the hopping algorithm, but cannot take place without violating the energy conservation, and are therefore given up. This

(25) Tully, J. C. *J. Chem. Phys.* **1990**, *93*, 1061.
(26) Tully, J. C. *Int. J. Quantum Chem. Synop.* **1991**, *25*, 299.
(27) Berendsen, H. J. C.; Grigera, J. R.; Straatsma, T. P. *J. Phys. Chem.* **1987**, *91*, 6269.
(28) Martí, J.; Guàrdia, E.; Padró, J. A. *J. Chem. Phys.* **1994**, *101*, 10883.
(29) Jorgensen, W. L. *Biochemical and Organic Simulation System* (*BOSS*), version 3.5, 1994.

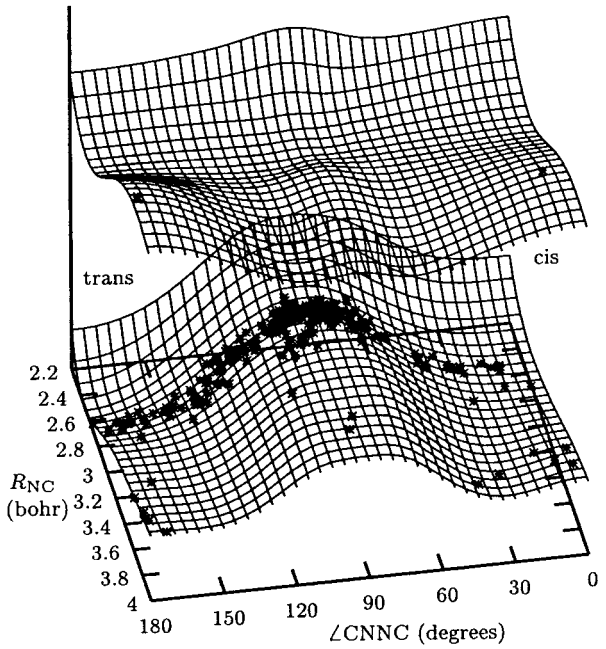

Figure 2. Photolysis of the isolated molecule, TSH simulation. ∠CNNC and R_{NC} coordinates for each trajectory at the time of the first surface hopping. The two PES are represented schematically (no geometry optimization) and the S_1 PES is shifted upward for a better view of the lower one.

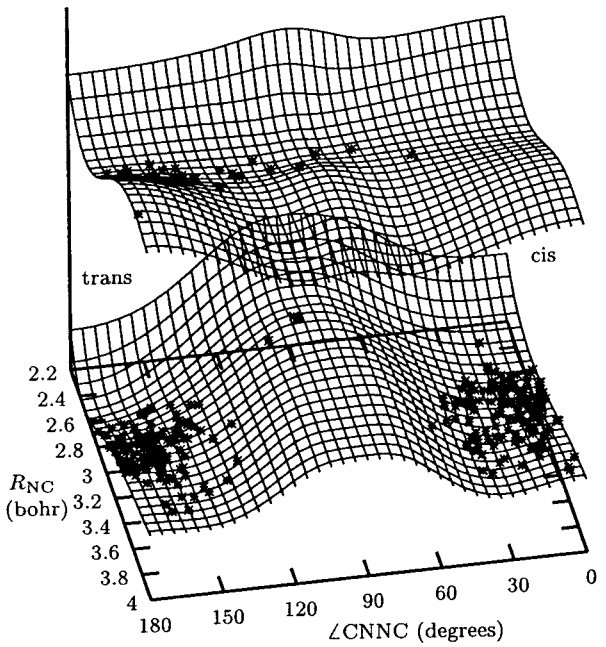

Figure 3. Photolysis of the isolated molecule, TSH simulation. ∠CNNC and R_{NC} coordinates for each trajectory at the time $t = 1$ ps. Same surfaces as in Figure 2.

problem is also met in our calculations, with $\langle P_1 \rangle$ showing a slower decay of the S_1 state with respect to N_1, after the first 200 fs. Despite this drawback, already detected in other dynamical situations,[13,14] Tully's algorithm compares well with fully quantum mechanical calculations performed by Müller and Stock[30] on a model of nonadiabatic isomerization. The azomethane molecule and Müller and Stock's model share an important feature, namely that the S_0-S_1 funnel is near to the minimum of the S_1 PES and to a high ridge for S_0: as a consequence, any trajectory (or quantum wave packet component) that hops to the ground state is not likely to pass again through the funnel, because of the multidimensional nuclear dynamics; moreover, even in the case of an upward transition from S_0 to S_1, the trajectory would be attracted again toward the funnel and eventually hop back to S_0. In the next sections we shall discuss the electronic decay on the basis of the N_K distributions, for consistency with quantum yields and energy disposal data, which are computed as fractions or histograms over all trajectories.

4. Photofragmentation of the Isolated Molecule

Figures 2 and 3 offer a sketchy view of the dynamics of an isolated *trans*-azomethane molecule, following the $n \rightarrow \pi^*$ excitation. The potential energy surfaces are represented as functions of ∠CNNC and R_{NC}, without optimization of the other coordinates. Each star indicates the position of a trajectory in the ∠CNNC/R_{NC} plane (the largest R_{NC} distance is always chosen). In Figure 2 we show the location of the first surface hopping, from S_1 to S_0; time is not the same for all trajectories, but in most cases it is less than 500 fs. Most of the surface hoppings occur near the bottom of the valley connecting the trans and cis isomers in the S_1 state, along the torsion coordinate, and especially between ∠CNNC = 60° and 120°, where the two PES are closest. Of course, nonadiabatic transitions require strong couplings and rather small energy gaps between the two surfaces, but it is not necessary to be very close to the crossing seam, so its exact location is not of paramount importance. Figure 3 shows the situation at 1 ps after the initial excitation. Most of the trajectories have settled in the ground state, close to the trans or cis isomer minima. Notice that we are running energy conserving dynamics for an isolated molecule: quite clearly, the excess energy which might enable the molecule to cross freely the potential barrier between the two isomers has been distributed among several other internal degrees of freedom. If this is true for azomethane, it must be a fortiori true for larger azoalkanes, with more vibrational modes.

The stochastic distribution of initial coordinates corresponds to a spread of excitation energies ΔE centered at 90 kcal/mol (i.e., λ=320 nm), with a Full Width at Half Maximum (fwhm) of 15 kcal/mol. This is in fair agreement with the position and spectral width of the $n \rightarrow \pi^*$ band.[31] In fact, we slightly overestimate the vertical transition energy (87 kcal/mol versus an experimental absorption maximum at 81 kcal/mol): this should be kept in mind when comparing our results with those of photodissociation experiments. Adding to ΔE the average vibrational energy prior to excitation, we have a total energy of 105 kcal/mol over the ground-state minimum, in principle more than enough to cause either sequential or symmetric fragmentation.

Quantitative results about the fate of the excited molecule are given in Figures 4 and 5. The former shows the short time dynamics, i.e., the decay of S_1, the isomerization and the initial formation of $CH_3NN^{\bullet} + CH_3^{\bullet}$ and $N_2 + 2CH_3^{\bullet}$. Figure 5 shows the long time dynamics (1−500 ps), which takes place almost entirely on the ground-state surface. Transitions from S_1 to S_0 do not occur before about 90 fs, the time needed to reach the strong coupling region. Plots of the ∠CNNC angle as a function of time (not here reported) show that, after a slower start, a trajectory can accomplish a complete oscillation or a revolution in the S_1 PES in about 100 fs. The lifetime of S_1 being of the order of 400 fs (see Figure 4), a few oscillations actually take place. Other coordinates undergo oscillations of smaller amplitude immediately after excitation: ∠NNC from about 105° to 140°, R_{NN} from 2.35 to 2.50 bohr, and R_{NC} from 2.5 to 3 bohr. The latter motion is more irregular than the other ones,

(30) Müller, U.; Stock, G. *J. Chem. Phys.* **1997**, *107*, 6230.

(31) Thompson, A. M.; Goswami, P. C.; Zimmermann, G. L. *J. Phys. Chem.* **1979**, *83*, 314.

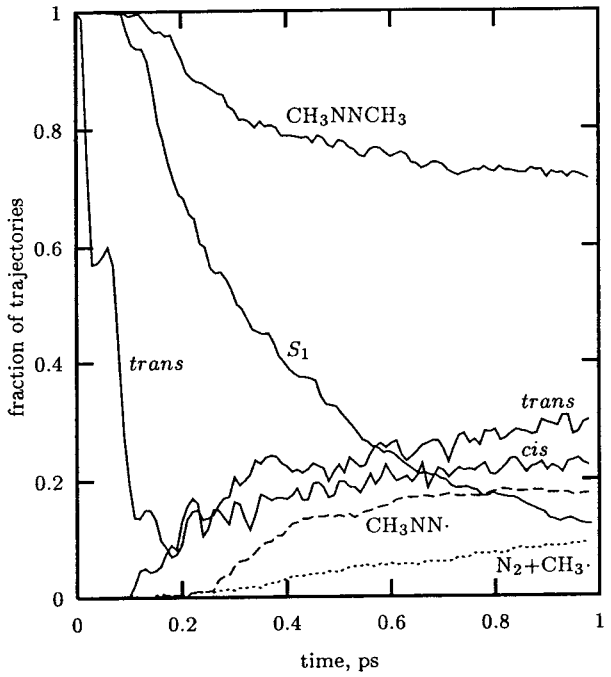

Figure 4. Photolysis of the isolated molecule (TSH simulation): short time dynamics. Fraction of molecules in various situations as functions of time. CH_3NNCH_3 molecules: both R_{NC} distances <4 bohr; cis conformation: $|\angle CNNC| < 30°$; trans: $|\angle CNNC - 180°| < 30°$; $CH_3NN^\bullet$ radical: one $R_{NC} > 8$ bohr, the other one <4 bohr; $N_2 + 2CH_3^\bullet$: both R_{NC} distances >8 bohr.

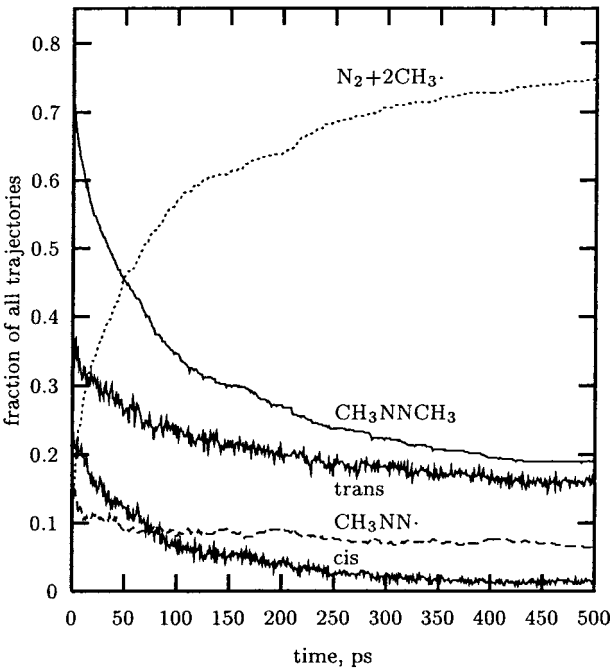

Figure 5. Photolysis of the isolated molecule, TSH simulation: long time dynamics. Fraction of molecules in various situations as functions of time, as in Figure 4.

because the two NC bonds do not elongate simultaneously: when one R_{NC} distance increases, the other one tends to remain short, both in S_1 and in S_0.

We set arbitrary boundaries on the internal coordinates, to monitor the occurrence of various molecular structures. Thus we have CH_3NNCH_3 when both NC distances are shorter than 4 bohr, and we distinguish the cis and trans isomers according to the value of $\angle CNNC$, which must be within 30° of 0 or 180°, respectively. At any time, the fractions of molecules in cis or trans situations sum up to slightly less than the total CH_3NNCH_3: just a few molecules do wander at intermediate angles. When one NC distance becomes longer than 8 bohr, and the other one is still shorter that 4 bohr, we have $CH_3NN^\bullet + CH_3^\bullet$. Most of the trajectories follow this route, while only 7% undergo simultaneous dissociation of both NC bonds in S_0 (i.e., both R_{NC} elongate beyond 8 bohr without ever meeting the $CH_3NN^\bullet$ condition). Only 4.4% of the trajectories dissociate directly on the S_1 PES, exclusively by the sequential mechanism, because S_1 correlates with a high lying state of N_2 along the symmetric dissociation path. The first excited state of $CH_3NN^\bullet$ prefers a collinear CNN geometry (C_{3v} symmetry), where it is degenerate with the ground state: therefore, nonadiabatic transitions occur during or just after dissociation and $CH_3NN^\bullet$ is eventually found in its ground state. The direct dissociation in S_1 and the simultaneous fragmentation mechanism in S_0 are fast processes (average lifetimes of 4 and 15 ps, respectively, with much shorter onset times), which occur preferably for the most energetic trajectories. In the short time range, also the one-bond dissociation in the S_0 PES contributes to the population of $CH_3NN^\bullet$, which reaches 18% around 1 ps, with an onset at about 250 fs. The rapidly formed $CH_3NN^\bullet$ also undergoes a fast fragmentation to $N_2 + CH_3^\bullet$. All these subpicosecond processes are quite clearly nonstatistical, in the sense that the internal energy has not yet been fully redistributed among all the vibrational modes (IVR process). Two distinct events, photon absorption and nonadiabatic deexcitation, deliver energy to selected subsets of internal modes. It is interesting to compare these results with those of our preliminary study,[10] based on a simplified model where the methyl groups were replaced by single masses, therefore eliminating several internal modes both of high and of low frequency. The agreement is good as far as short time dynamics is concerned, in particular the nonadiabatic decay; however, fragmentation was overall much faster, and with a larger proportion of simultaneous two-bond dissociation.

Most trajectories are still undissociated after 1 ps, and they rapidly settle either in the cis or in the trans minimum. The randomization of the vibrational energy distribution inhibits the processes with higher energy barriers, isomerization, and simultaneous fragmentation. Therefore, the cis and trans populations evolve almost separately, steadily decreasing because of one-bond dissociation. The cis isomer dissociates faster than the trans one, because of its smaller bond energy. Moreover, the decay is faster in the first 100 ps (corresponding to lifetimes of about 80 and 350 ps for cis and trans, respectively) and slower afterward (lifetimes of 300 and 900 ps). The nonexponential form of the decay reflects the distribution of excitation energies: higher energies cause faster dissociation, the unimolecular reaction rate increasing by a factor of 2 when moving upward by 10 kcal/mol in the energy (remember that the fwhm of our energy spread is 15 kcal/mol). $CH_3NN^\bullet$ is formed with a large excess of internal energy, about 31 kcal/mol, therefore it dissociates in a time shorter than azomethane itself, of the order of 10 ps. This value may be overestimated if the potential barrier opposing $CH_3NN^\bullet$ dissociation is indeed lower than we computed.[8,23] As a result, a low, almost steady-state, population of $CH_3NN^\bullet$ is predicted by our simulation, while N_2 is produced at a rate approximately matching the decay of CH_3NNCH_3 (Figure 5).

We can now compare our results with those of Lee's and Zewail's experiments.[4,7] Our view is that Zewail's group monitored the short time dynamics, i.e., fast formation and decay of $CH_3NN^\bullet$, partly by direct dissociation in the S_1 PES, and

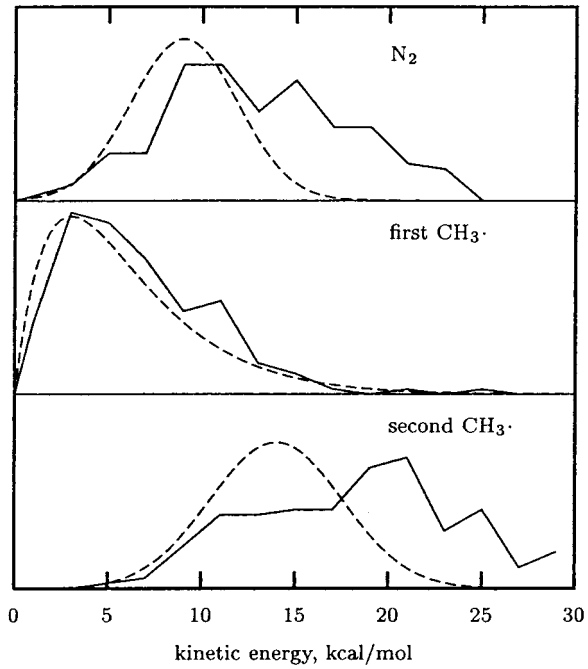

Figure 6. Photolysis of the isolated molecule, TSH simulation. Selection of trajectories with excitation energy $\Delta E < 92$ kcal/mol. Full lines: Computed kinetic energy distributions for N_2, for the first and for the second leaving $CH_3^\bullet$ fragment. The first $CH_3^\bullet$ is the one that has travelled further from the center of mass upon complete fragmentation (both R_{NC} distances >8 bohr). Dashed lines: Experimental results.[4]

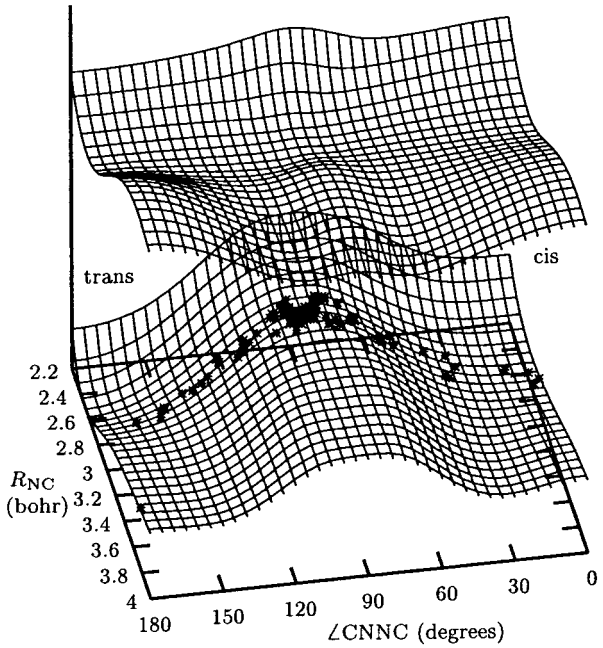

Figure 7. Photolysis in water solution, MDSH simulation. ∠CNNC and R_{NC} coordinates for each trajectory at the time of the first surface hopping. Same surfaces as in Figure 2.

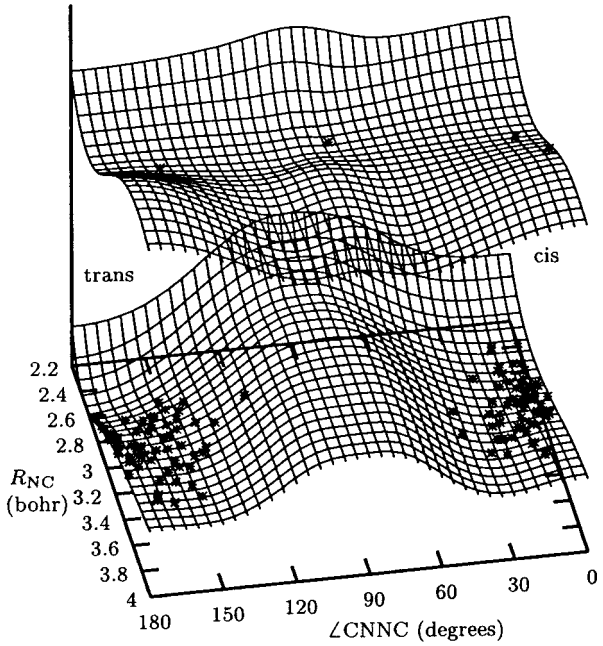

Figure 8. Photolysis in water solution, MDSH simulation. ∠CNNC and R_{NC} coordinates for each trajectory at the time $t = 1$ ps. Same surfaces as in Figure 2.

prior to the statistical redistribution of vibrational energy in the ground state; they measured rise and decay times somewhat shorter then we have computed, partly because they used a photon energy of 92.2 kcal/mol (about 12 kcal/mol above that of the absorption maximum). Lee's experiment was done with a photon energy of 81.4 kcal/mol, almost coincident with the absorption maximum, and concentrated on the vectorial properties of the fragment velocities. According to our simulations, about 70% of the dissociation events occur with times longer than 1 ps; this slower part of the reaction dynamics goes through the sequential steps of decay to S_0, isomerization or reversion to the trans minimum, and dissociation to $CH_3NN^\bullet + CH_3^\bullet$ and then to $N_2 + 2CH_3^\bullet$, and this mechanism has the largest influence on the fragment velocity distributions. On the basis of their measurements, Lee and co-workers attributed a long average lifetime to CH_3NNCH_3, which is not in contrast with Zewail's finding that some degree of prompt fragmentation occurs. On the other hand, both Lee's and Zewail's estimates of the $CH_3NN^\bullet$ lifetime are shorter than ours, which confirms that the activation energy for $CH_3NN^\bullet$ dissociation is lower than we computed.

For a closer comparison of our simulations with Lee's results, we computed translational kinetic energy distributions of N_2 and $CH_3^\bullet$. We selected only trajectories with excitation energies between 74 and 89 kcal/mol, an interval centered about the photon energy used in the experiments. For each trajectory, we distinguish the methyl group which dissociates first from the second one, to verify Lee's assumption that the methyl fragments originated from CH_3NNCH_3 and from $CH_3NN^\bullet$ are responsible respectively for the low and high energy peaks in the distribution. Figure 6 shows that this is indeed the case. The agreement with the experimental results is quite good for the "first" $CH_3^\bullet$ fragment, while the kinetic energies of N_2 and of the "second" $CH_3^\bullet$ are slightly overestimated. The discrepancy is due in part to the fact that a fraction of trajectories have not yet reached dissociation after 500 ps (still 19% of azomethane and 7.5% of $CH_3NN^\bullet$), with a bias toward the less energetic ones; and, in part, it is another manifestation of the overestimated energy barrier between $CH_3NN^\bullet$ and $N_2 + CH_3^\bullet$.

5. Photochemistry in Solution

Figures 7 and 8 are analogous to Figures 2 and 3 for the photolysis of azomethane in aqueous solution. Comparing Figures 2 and 7 one sees that surface hopping occurs essentially at the same geometries; the MDSH simulation only shows a slightly higher selectivity for the strong coupling region around ∠CNNC = 90°. The overall picture of the short time dynamics

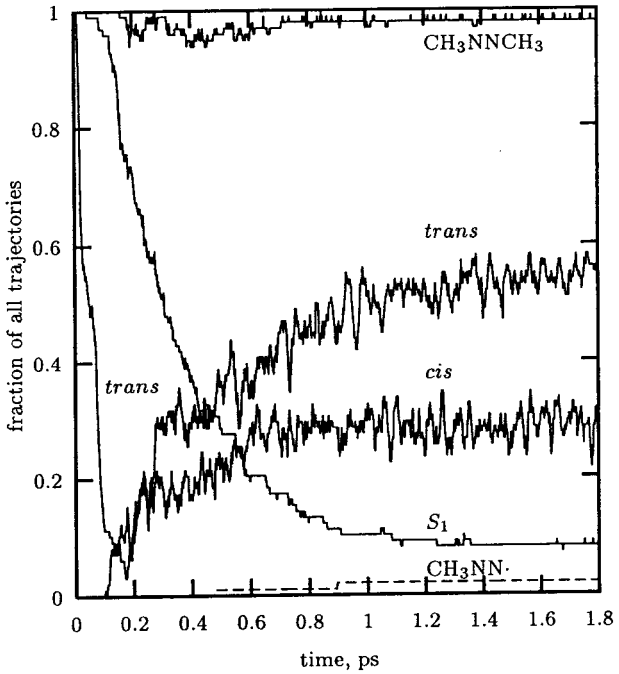

Figure 9. Photolysis in water solution, MDSH simulation. Fraction of molecules in various situations as functions of time, as in Figure 4.

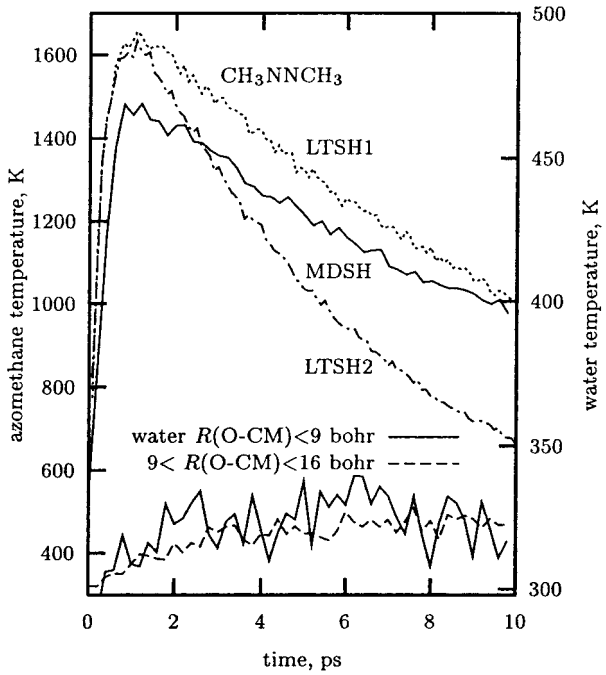

Figure 10. Photolysis in water solution, MDSH simulation. Kinetic energy of azomethane, of water molecules with the O atom within 9 bohr of the center of mass of CH_3NNCH_3, and of an outer shell of water (distance between 9 and 16 bohr), as functions of time. LTSH1 and LTSH2 label the kinetic energy of azomethane obtained in Langevin trajectory surface hopping calculations with different friction coefficients. All kinetic energies are expressed as equivalent temperatures ($T = 2E_K/(3NK_B)$, where N is the number of atoms. Notice that different scales are used for azomethane and for water temperatures (left and right axis).

remains the same as in vacuo: fast internal conversion and isomerization, with only small quantitative differences which can be appreciated by looking at the populations as functions of time (Figure 9). In fact, the lifetime of the excited state is unchanged, while after 1 or 2 ps a larger fraction of trajectories can be classified as either cis or trans, according to the criteria seen above. Quite clearly, the transfer of vibrational energy to the solvent tends to confine the solute molecules in the regions of the relative minima. In the same time interval, the trans to cis ratio is higher for the photolysis in water, showing that also in the excited state there is a more pronounced preference for the region of minimum energy, which is on the transoid side ($\angle$CNNC $\simeq$ 130°). Eventually, when all trajectories have reached the ground state, the quantum yield of the trans−cis isomerization is 36%. This value can be compared with $\Phi = 0.42$, obtained experimentally in benzene,[1] with $\lambda = 365$ nm.

The really important new feature of azomethane photochemistry in solution, with respect to the gas phase, is the almost complete suppression of fragmentation: experimentally, a quantum yield of 1% is found in water, with $\lambda = 365$ nm. In the MDSH simulations, 2% of the trajectories reach dissociation to $CH_3NN^{\bullet} + CH_3^{\bullet}$: of course, given the small numbers involved, the statistics here are very poor. The inhibition of dissociation is not due to specific interactions with the solvent, which may hinder some particular internal motions of the solute. In fact, the initial oscillations of the skeletal coordinates are quite similar to those found in vacuo, and have the same amplitudes. However, vibrational energy is efficiently transferred to the solvent, at a rate competing with fragmentation. To quantify the energy flow, we have computed the kinetic energy of azomethane and of two shells of water molecules, selected according to the distance R(O−CM) between the O atom and the center of mass of CH_3NNCH_3: those with R(O − CM) < 9 bohr (about 10 molecules) and those with 9 < R(O − CM) < 16 bohr (about 60 molecules). Figure 10 shows the kinetic energies E_K as functions of time; to make them directly comparable, we have expressed them as absolute temperatures $T = 2E_K/(3NK_B)$, where N is the number of atoms and K_B the Boltzmann constant. The kinetic energy of azomethane increases sharply during the first picosecond, when the molecule gathers momentum sloping down the S_1 surface, and much more as a consequence of the decay to S_0. The energy transfer to water is fast: it corresponds to an exponential time constant of about 16 ps. Compared with the long dissociation times we find in vacuo (see preceding section), and taking into account that the unimolecular dissociation rate depends sharply on the excess energy, this seems a sufficient explanation of the "cage effect".

In Figure 10, the MDSH result is compared with two Langevin trajectory surface hopping (LTSH1 and LTSH2) simulations[32] using different friction coefficients (twice as large for LTSH2 as for LTSH1). While qualitatively the behavior is the same for MDSH and LTSH, we see that according to the MDSH model the energy transfer is comparatively more efficient in the short time range (2−3 ps) and slower afterward. This is an effect of the frequency dependence of the coupling between solute and solvent modes: low frequency, large amplitude motions of the solute, such as double bond torsion, N-inversion, and NC bond elongation, transfer energy to the solvent more efficiently than others. Such energy wasting motions prevail in the first picoseconds after excitation, while afterward the internal energy of azomethane is rapidly redistributed among all modes. Of course, such details are totally ignored in Langevin dynamics with time-independent friction coefficients.[32]

The heating of surrounding water molecules is modest: for the 10 closest molecules we find larger fluctuations, up to 40 K above the equilibrium temperature (298 K), very rapidly damped; the outer shell of 60 molecules warms more regularly,

(32) Cattaneo, P.; Granucci, G.; Persico, M. *J. Phys. Chem. A* **1999**, *103*, 3364.

by about 25 K. This is in line with the macroscopic thermal conductivity and specific heat of water. These results show that, if the solute to solvent energy loss is fast, the energy flow toward outer solvation shells is even faster, and reaches the boundaries of the cell within the time of our simulation. Of course a larger cell would allow us to simulate more correctly the long range energy flow, but the small temperature increase we observe cannot affect significantly the photochemical dynamics. In fact, we also ran simulations where the kinetic energy is rescaled at each step, to give an average value in line with the equilibrium temperature. While the theoretical framework of such a procedure is less satisfactory than that of energy conserving simulations, the results are quite similar.

6. Conclusions

To our knowledge, this study presents the first simulation of condensed-phase photochemistry, with a realistic model of the solvent and of a polyatomic solute, compared with the corresponding gas-phase dynamics.

Our results show that the photofragmentation of azomethane in vacuo goes prevalently through the following steps: fast internal conversion (<0.5 ps), isomerization or reversion to the trans form (about 1 ps), dissociation of the first NC bond to form the methyldiazenyl radical (80−900 ps), and rapid fragmentation of $CH_3NN^{\bullet}$ to $N_2 + CH_3^{\bullet}$. About 80% of the excited molecules follow this pathway, but smaller fractions produce methyldiazenyl in much shorter times (<1 ps), either in the ground state, prctically without undergoing isomerization or IVR, or directly on the excited-state PES. The prompt dissociation mechanism and even some degree of simultaneous fragmentation to $N_2 + 2CH_3^{\bullet}$ become more important when increasing the photon energy. These findings help to solve the apparent contradiction between experimental results by Lee's and Zewail's groups, who found evidence of slow and fast dissociation, respectively, by using different techniques.[4,7]

The simulation of photolysis in water solution shows that the S_1 to S_0 decay and the trans to cis isomerization are only marginally influenced by solvent effects, while the vibrational energy transfer to the surrounding water molecules competes effectively with dissociation, which is largely suppressed. The energy flow through the solvent is even faster than the energy loss of the solute, therefore the local heating of the first solvation shell is quite moderate and does not affect significantly the photoreaction dynamics.

Acknowledgment. This work was supported by grants from the Italian MURST and by the CNR Dynamics, reactivity and structure of molecular solutes project.

JA0102843